Internship Report

Analysis of infrared thermography data from edge probe experiments at the W7-X stellarator

Aloïs Coquillard
Département de Physique, M1 SdM
École Normale Supérieure de Lyon
Année 2025–2026

Carried out at
Max Planck Institut
Für Plasmaphysik
Teilinstitut Greifswald
Wendelsteinstraße 1
https://www.ipp.mpg.de

Supervised by
Carsten Killer
Gruppe E5 – Stellarator-Dynamik und -Transport
tel. 03834 88 2228
carsten.killer@ipp.mpg.de

Abstract

The objective of this internship was to study an infrared camera view of the Langmuir probe **FLUC 3** inside the W7-X stellarator in order to infer information about the heatfluxes it was subject to. Compared with the direct Langmuir probe measurements, it would give valuable information about edge plasma physics of W7-X geometry, specifically magnetic islands.

Keywords: *Langmuir probe, IR thermography, thermal modeling, stellarator, W7-X*

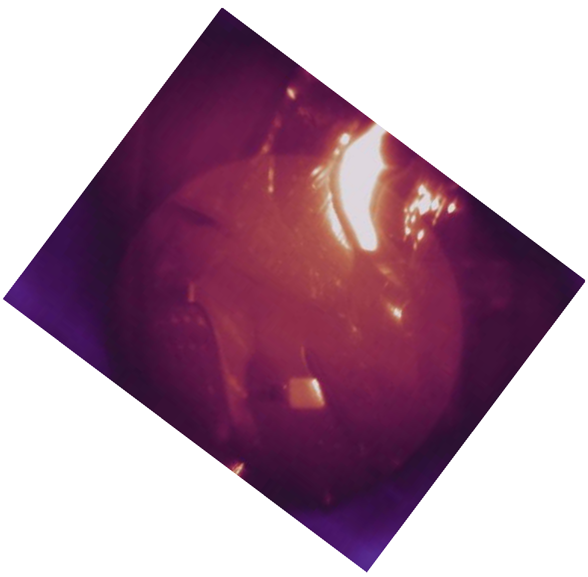

Acknowledgements

I would like to thank the IPP E5 department team for warmly welcoming me during this internship, as well as for providing the resources that helped me through the many times I found myself lost in the infrastructure.

I would also like to thank Frédéric Brochard, CNRS researcher in fusion plasmas at the Institut Jean Lamour in Nancy and supervisor of my previous internship, who introduced me to the incredible world of stellarators and without whom I would never have found this great research opportunity.

Among my fellow interns at IPP, I would like to thank Alice, Tomai, Nassim, Ian and all the others I had the opportunity to meet, who supported me throughout this journey. I am equally grateful to the physicists and engineers who were kind enough to spare their time to share their knowledge — and cheerfulness! — with me.

Finally, I would like to express my gratitude to Carsten Killer, whose availability, enthusiasm, and kindness made this internship not only an unforgettable learning experience, but also a truly enjoyable one.

Table of content

I Introduction

Plasma, often referred to as the fourth state of matter, is widely studied due to its many applications, notably in nuclear fusion. Controlled fusion would enable the production of clean and sustainable energy by reproducing the processes occurring in the Sun. Despite decades of progress and major international efforts such as ITER, achieving efficient and stable fusion remains a major scientific challenge.

A key difficulty lies in plasma stability. Even when appearing stable, magnetically confined plasmas are affected by small-scale instabilities that can cause turbulence and degrade confinement. In **tokamaks**, this can result in **disruptions** of the plasma current required to confine it, causing a sudden and violent loss of confinement.

Stellarators offer an alternative approach, relying entirely on externally generated magnetic fields and thus avoiding large plasma currents. This makes them inherently more stable and suitable for a steady-state operation. The **Wendelstein 7-X** (W7-X) stellarator, located at the Max Planck Institute for Plasma Physics in Greifswald, Germany, is the world's largest optimized stellarator and a leading experiment in this field, aiming to demonstrate that optimized magnetic configurations can achieve stable, high-performance confinement.

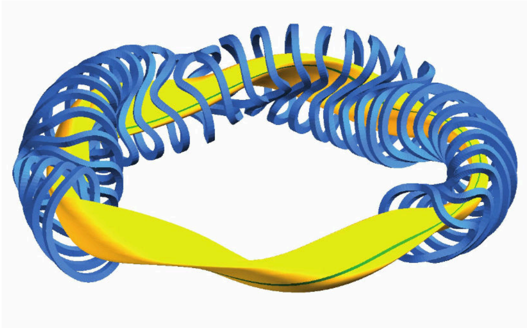

Figure 1: The coils geometry of W7-X stellarator.

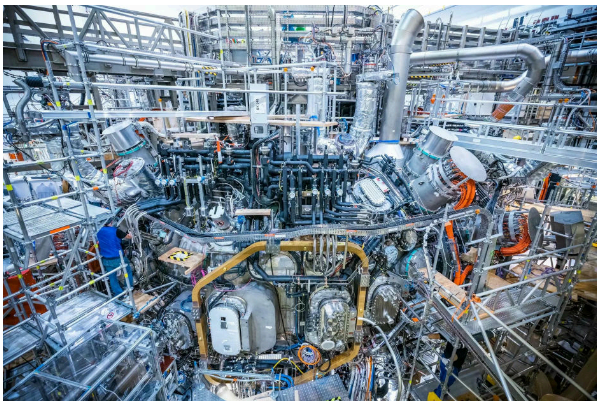

Figure 2: The Wendelstein 7-X stellarator experiment.

In this context, understanding how heat and particles escape confinement and interact with the surrounding material walls is one of the central open problems of fusion research. These plasma–wall interactions determine both the performance and the longevity of future reactors, and studying them requires dedicated diagnostics capable of providing simultaneous local measurements of temperature, density, and heat flux in the harsh edge environment (high temp., turbulent, MJ/m^2). Addressing this typically means combining complementary diagnostics, such as fast local probes and thermal imaging, and reconciling them — the kind of problem this internship sets out to work on.

The **Max Planck Institut für Plasmaphysik** (IPP) in Greifswald, as the host institution of W7-X, is one of the world's leading centers for plasma edge physics and plasma diagnostics. W7-X's magnetic divertor islands — a geometry specific to stellarators — offers a reproducible and disruption-free environment that is particularly well suited to edge transport studies, while still not perfectly understood yet. The amount of experimental diagnostics deployed around W7-X, and the expertise of the teams operating them, made IPP Greifswald a compelling destination to explore these questions during an M1 internship.

Figure 3: The Max Planck Institut für Plasmaphysik complex at Greifswald, with the W7-X building on the left.

Appendices

A. Theory of stellarators and W7-X specificities

Stellarators, even though less well-known than their tokamak counterparts, belong to the same family of nuclear reactors and are in fact an older design. Like tokamaks (of which ITER is an example), their objective is to produce fusion reactions by confining the necessary plasma with strong magnetic fields.

A.1 History

Since the discovery of fusion in 1934 by Oliphant, Harteck and Rutherford [4], the idea of harvesting its power has been in many minds. The reaction with the lowest activation energy is deuterium–tritium at around 100 keV, and most setups have been engineered around this reaction. This energy corresponds to a thermal agitation of billions of Kelvin — no known material can withstand such temperatures. Fermi showed [5] that, due to the Boltzmann distribution, the reaction was still feasible at around 50 million degrees, but a specific setup for containing the heat and the particles was needed.

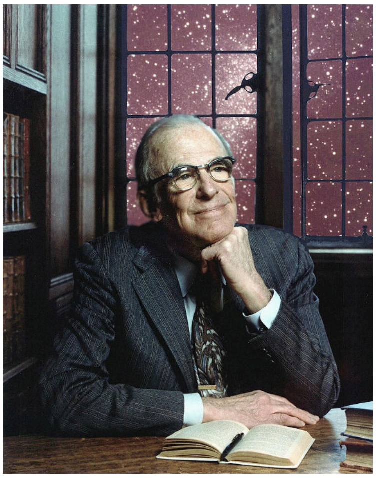

Figure 33: Lyman Spitzer, creator of the stellarator concept.

Because at these temperatures plasmas are fully ionized, it is technically possible to confine them using electromagnetic fields, but their arrangement was anything but trivial. After multiple fruitless experiments using electric fields or acoustic waves, the first viable concept came from American scientist Lyman Spitzer in 1951 [6], also known for being one of the first to propose the idea of space telescopes.

Spitzer's *stellarator* is a toroidal reactor where the plasma is kept in a donut shape by external coils. To compensate for the curvature of the magnetic field, which tends to separate ions and electrons and create dangerous electric fields, Spitzer proposed twisting the field lines so that the drift alternates direction and averages to zero over one full revolution. In his original design this was achieved by bending the torus into a figure-8; later designs replaced this with helical coil windings around a single ring.

In parallel to this work, the idea of a simpler reactor, the *tokamak*, was developped in the USSR by Andrei Sakharov, father of the soviet atomic bomb. This concept would reveal to have better results than the contemporary stellarators and shift the focus of most researchers into tokamak theory in the 1970s.

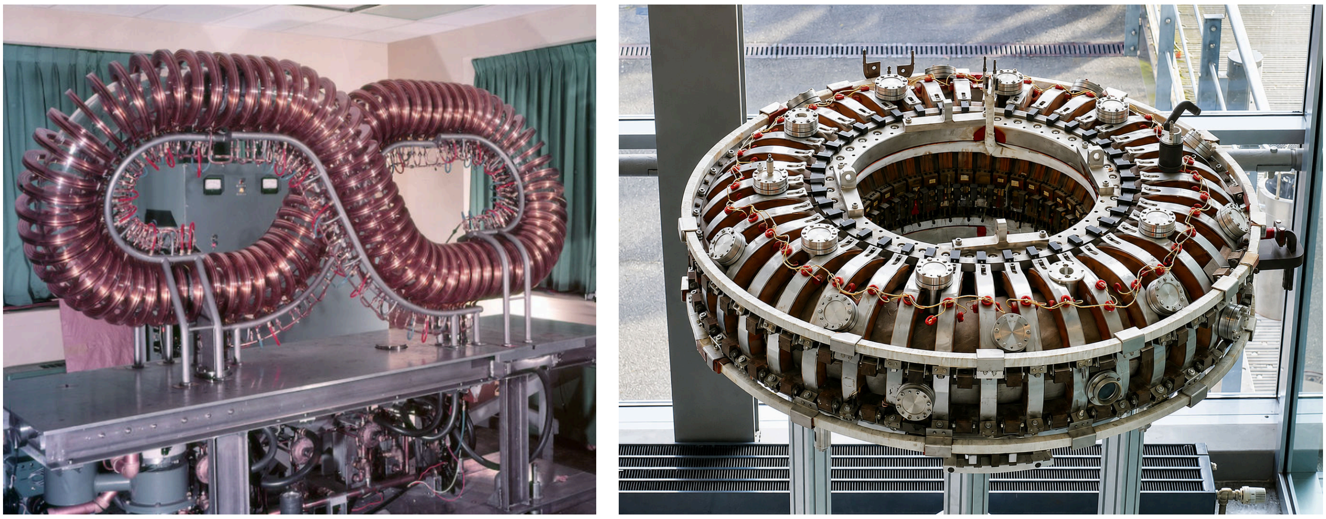

Figure 34: On the left: a figure-8 stellarator prototype from 1958 made by the Princeton Plasma Physics Laboratory. On the right: Wendelstein-II B, early toroidal stellarator with helical coils now exposed at the entrance of the Greifswald IPP.

This shift culminated in the ITER project — an international reactor-scale tokamak under construction in Cadarache, France, agreed upon in 1985. Meanwhile, advances in numerical optimisation in the 1990s breathed new life into the stellarator approach: the Large Helical Device (LHD) in Japan achieved first plasma in 1998, and the W7-X project, conceived at IPP Greifswald in the same period, achieved first plasma in December 2015, becoming the world's leading stellarator research platform.

A.2 Main differences with tokamaks

Both devices use a helical magnetic field in a toroidal geometry; the particles follow the magnetic lines which themselves helically rotate toroïdally. The difference however lies in how the field is twisted. In a tokamak, the poloidal component is generated by a large current driven through the plasma itself, making the device inherently pulsed and prone to sudden disruptions: violent losses of confinement that can deposit megajoules on the first wall in milliseconds. In a stellarator the full field is generated by external coils only, eliminating disruptions and allowing steady-state operation, at the cost of a far more complex coil geometry.

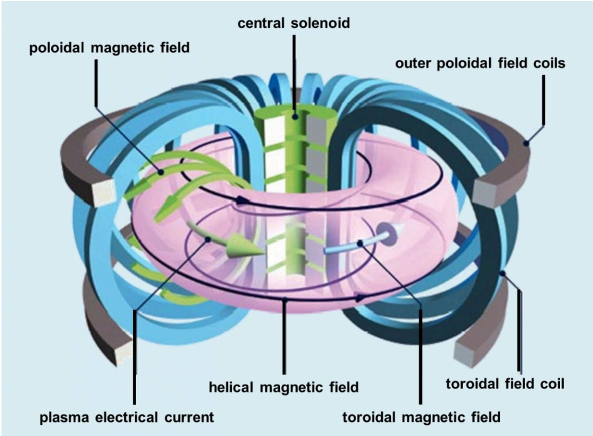

Figure 35: Geometry of a tokamak.

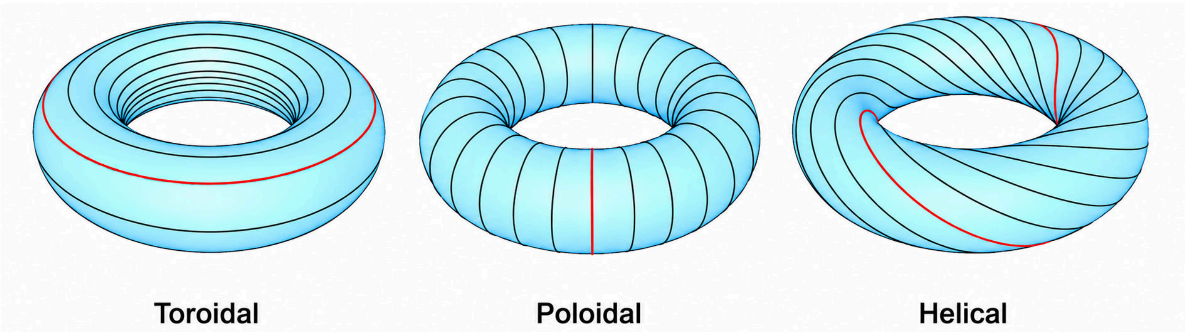

Figure 36: The different types of field lines inside a torus. To achieve an helical magnetic field, either complex 3D coils (modern stellarators) or a mix of poloidal and helical coils (tokamaks) must be used concomitantly.

A.3 Design possibilities and W7-X geometry

A.3.a 3D coils

The freedom to shape the magnetic coils in three dimensions opens a vast optimization space unavailable to axisymmetric devices like tokamaks. The key quantity to optimise is collisionless particle transport: in a curved magnetic field, some particles can be trapped in local magnetic field minima — analogous to a ball caught in a potential well, technical term is *magnetic mirror* — and their guiding-centre drifts then carry them slowly outward, leaking energy out of the plasma. In a tokamak, toroidal symmetry guarantees an exact conservation law that prevents this radial drift entirely. A generic stellarator, lacking this symmetry, can suffer far higher losses through this mechanism.

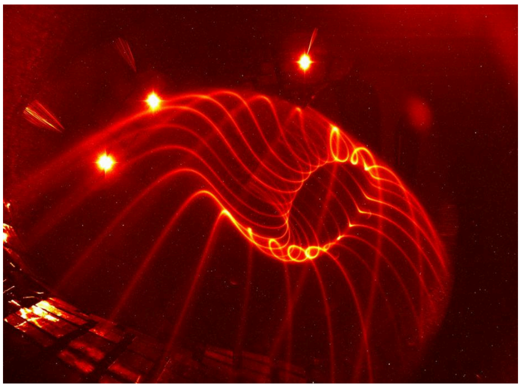
Figure 37: Magnetic field lines inside W7-X, traced by a fluorescent electron beam [7].

The goal of W7-X's design was to find a three-dimensional coil shape whose field geometry mimics this protective property without needing full symmetry — achieving through careful engineering what tokamaks get for free from their shape. This was done through intensive numerical optimisation, and realised with 50 superconducting non-planar coils in five identical modules (see part I for an image), together with planar and trim coils that allow the configuration to be varied between shots [8].

A.3.b Divertor islands

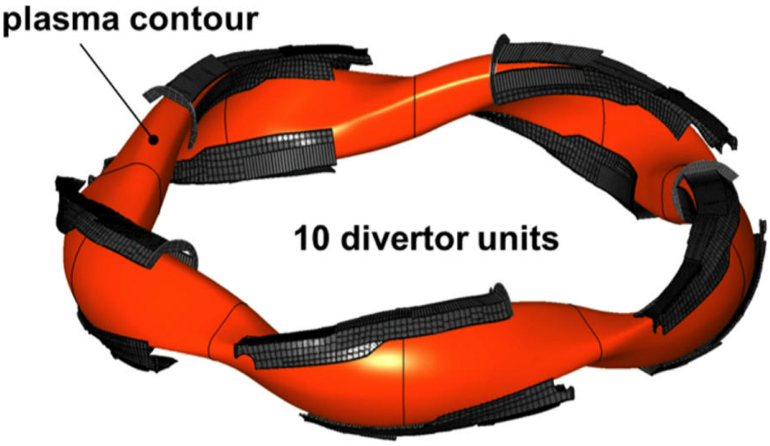

Figure 38: The 10 island divertor units (dark target plates) positioned around the W7-X plasma volume (orange) [9].

Any fusion device also needs a way to exhaust the heat and particles that continuously leak out of the confinement region, otherwise the vessel walls would be eroded in seconds. This is the role of the ***divertor***: a set of armoured target plates positioned where the escaping field lines strike, designed to absorb the heat load and remove the spent fuel; these would be the main sources of energy for the steam generator in a power plant. In a tokamak, toroidal symmetry has been engineered so that it produces a single continuous divertor ring at the bottom of the vessel.

In W7-X, the non-axisymmetric field creates a richer structure at the plasma boundary: instead of closing smoothly, the outermost field lines form a chain of five interlocked *magnetic islands* — regions where the field lines retrace their path after a fixed number of revolutions around the torus, creating a natural boundary between the confined plasma and the vessel wall. These islands concentrate the escaping power on well-defined zones on the vessel wall. The W7-X *island divertor* consists of 10 graphite target units, two per $\frac{2\pi}{5}$ section, positioned precisely where the island field lines converge onto the vessel wall [9].

A.3.c Naming the magnetic configurations

Each experiment runs in one of several dozen pre-computed magnetic configurations, identified by a short letter code. These codes place a configuration along three knobs: the *rotational transform* (*iota*, how many times a field line winds poloidally per toroidal turn), the *mirror ratio* (how strongly particles are trapped locally, from how much the field strength varies along a field line), and the *magnetic shear* (how much iota varies across the plasma). The main configurations used in W7-X are:

Regime	**Configurations**	**Regime**	**Configurations**
Low iota	DAM, DBM	High iota	FTM
Standard	EIM	High mirror	KJM, KKM
Std. → low iota	EBM, ECM, EEM, EGM, EHM	High mirror, high iota	KNM, KLM
Std. → high iota	FMM, FNM, FLM	Low shear	DKJ, IKJ, MMG, KOF
Negative mirror	XIM	High shear	DIR

A.4 Personal opinion : why stellarators are probably the future

I was quite astonished when I learned a year ago during my previous internship about stellarators and their advantages/caveats; while tokamaks are quite well-known from the public, this other solution to achieve fusion as a power source doesn't have the media coverage it deserves.

After working at the IPP for a few months, I can now confirm to myself how relevant stellarator research is, thanks to its many advantages (24/7 operation, no disruption issues, etc.) that, when finally mastered by current research, will make it not only an ideal candidate for a power plant, but a superior option to a tokamak by a large margin.

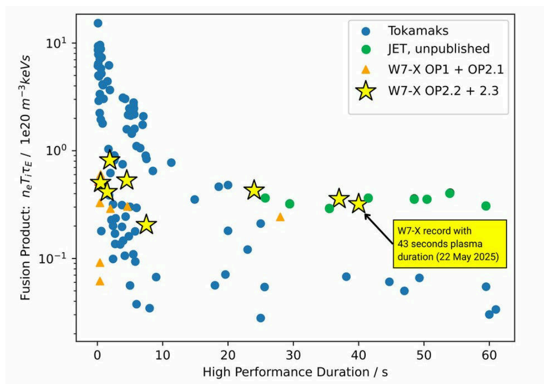

Figure 39: Wendelstein 7-X fusion performance vs pulse duration, compared to modern tokamaks.

Tokamak research like the ITER project will still be quite useful for understanding fusion plasma physics in the futur and still need to happen, but a shift in the scientific community seems have started in the last years toward stellarator research, and I think it is for the better.

B. Langmuir probes theory

This appendix gives a non-exhaustive description of how so-called *Langmuir probes* can be used to measure several plasma parameters. It is adapted from a similar appendix of my previous internship report, enriched with details specific to multiprobes setups like those I've worked on with IPP FLUC 3.

B.1 Classic Langmuir probes

Description. The Langmuir probe is a fundamental tool for the local diagnostic of weakly as well as highly ionized plasmas. It gives access to several essential plasma quantities, such as the electron density n_e, the electron temperature T_e, the plasma potential V_p, and, under certain conditions, the ion density and temperature.

The basic setup consists of a conductive electrode (typically a metallic rod) inserted into the plasma, to which a variable voltage V is applied relative to a reference (often the confinement vessel, acting as ground). The probe then collects a current I that depends on the applied voltage, which makes it possible to trace a current-voltage characteristic $I(V)$.

Operating principle. The principle relies on the mechanisms of selective collection of charged particles: by sweeping the probe voltage from a strongly negative to a strongly positive regime, one successively explores different collection regimes. For potentials strongly negative with respect to the plasma, the probe repels electrons and collects essentially ions: this is the *ion saturation regime*. As the voltage increases, a growing fraction of the plasma electrons have enough energy to reach the probe, leading to an exponential increase of the electron current; this is the *transition regime*. Once a certain potential, called the *plasma potential* V_p, is reached, all available electrons are collected: this is the *electron saturation*.

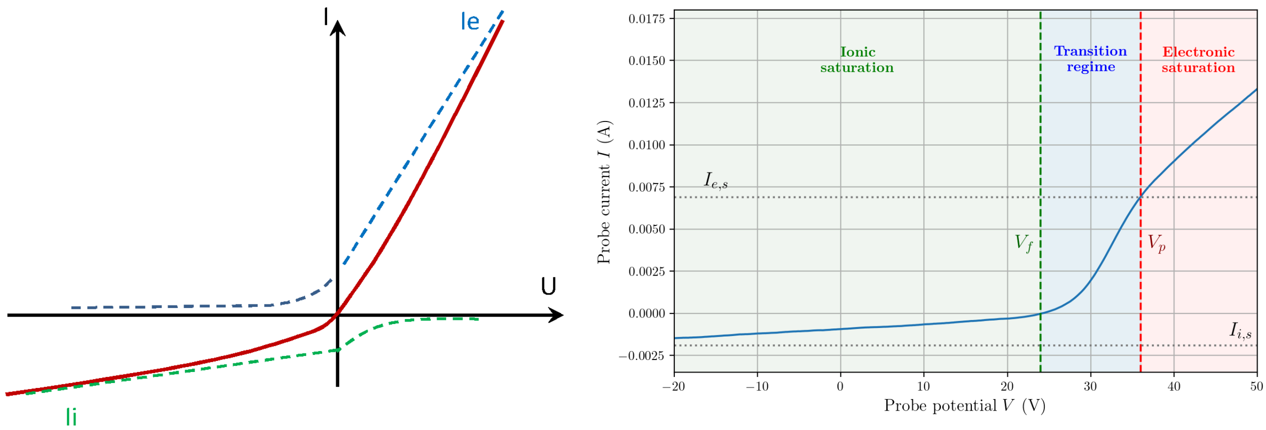

Figure 40: Left: current-voltage characteristic curve of a Langmuir probe, with the respective contributions of I_i and I_e. Right: example of a probe characteristic, redrawn from a measurement taken on the Aline cold plasma device during a previous internship at the Jean Lamour Institut in Nancy, France.

It has been shown in [10] how these different regimes operate. Assuming a Maxwellian distribution of the electron and ion velocities, one can derive the fraction that will be fast enough to reach the probe for a given potential. The formulas are:

$$I_e(V) = I_{\text{e,s}} \exp\left(\frac{e(V - V_p)}{k_B T_e}\right) \quad \text{and} \quad I_i(V) \approx I_{\text{i,s}} \quad \text{if} \quad V \leq V_f \tag{4}$$

where $I_{\text{e,s}}$ and $I_{\text{i,s}}$ are the electron and ion saturation currents, V_p the plasma potential, k_B the Boltzmann constant, T_e the electron temperature, and e the elementary charge. V_f is the floating potential, i.e. the potential at which the electron and ion currents cancel out ($I = 0$). The saturation currents are likewise well defined and proportional to the respective density of each species:

$$I_{\text{e,s}} = eSn_e\sqrt{k_B \frac{T_e}{2\pi m_e}} \quad \text{and} \quad I_{\text{i,s}} = -eSn_i\sqrt{k_B \frac{T_i}{2\pi m_i}} \tag{5}$$

where S is the collecting surface of the probe, T_e and T_i are respectively the electron and ion temperatures[8], and m_e and m_i are the electron and ion masses respectively.

Deviations from practice. The theory given in the previous paragraph implies that for $V \geq V_p$, a plateau equal to the collection of $I_{\mathrm{e,s}}$ should be reached. However, other phenomena, not discussed here, cause I to keep increasing even past this point. The plasma potential then only becomes identifiable as the abscissa of a slight inflection point of the curve, as can be seen in the figure above. In the case of the measurements on Aline (during the author's previous internship), identifying this inflection point was sometimes a challenge, leading to measurements that were often unusable for computing V_p.

B.2 Multi-pin and other Langmuir probes setups

Multi-pin (triple-probe) measurements. Sweeping the voltage of a single probe, as described above, requires the plasma to stay stationary over the whole duration of the sweep, and only probes one location at a time. Neither assumption holds for the Fluc 3 probe used in this internship: its 29 pins are meant to resolve the heat-flux pattern simultaneously across the whole probe head, in a turbulent, fast-fluctuating edge plasma, during a single brief plunge of the manipulator arm (see Section II.1).

The *triple-probe* technique [11] removes the need for a voltage sweep entirely by combining three simultaneous single-point measurements instead of one sweep. Two pins are tied together through a fixed external bias V_d: the first is driven far enough into negative territory to sit in pure ion saturation ($I_1 = -I_{\mathrm{i,s}}$), while the second, held at the fixed potential $V_2 = V_1 + V_d$, shares a closed current loop with the first — current conservation in that loop then forces $I_2 = +I_{\mathrm{i,s}}$. The third pin is left entirely floating and simply reads V_f. Writing the exponential collection law given above for pin 2 and imposing $I_2 = +I_{\mathrm{i,s}}$ collapses to a single closed-form relation:

$$k_B T_e = \frac{e\left(V_2 - V_f\right)}{\ln(2)} \tag{6}$$

so that T_e is obtained instantaneously from two potential readings alone, without ever varying the bias. The ion saturation current $I_{\mathrm{i,s}}$ is read directly off the first pin, and combined with T_e in the saturation-current relation given above to recover the electron density n_e (assuming quasineutrality, $n_e \approx n_i$).

This is exactly the arrangement used on each of FLUC 3's five triple-probe groups — one pin biased positively, one negatively, and one left floating (Section II.1) — letting T_e and $I_{\mathrm{i,s}}$, and therefore the Bohm heat flux, be recovered continuously and simultaneously at five poloidal positions across the probe head during a single plunge. The price paid for this speed is the assumption that T_e and the plasma potential stay uniform over the small spacing between the three pins of a given triple, an assumption the single-sweep method above does not need to make.

Ion saturation current. The expression for $I_{\mathrm{i,s}}$ given in the classic theory above — a thermal flux scaling with $\sqrt{T_i}$ — necessitates a correction in the conditions of a fusion edge plasma. There, the probe is surrounded by a thin positively charged layer, the *sheath*, and the Bohm criterion [12] states that ions cannot enter it slower than the ion sound speed

$$c_s = \sqrt{\frac{k_B(T_e + T_i)}{m_i}} \approx \sqrt{\frac{2k_B T_e}{m_i}} \quad \text{for } T_i \approx T_e, \tag{7}$$

so that the ion flux collected in saturation is set by T_e (through the sheath) rather than by the ions' own temperature:

$$I_{\mathrm{i,s}} \approx \alpha\, e\, n_e c_s S \tag{8}$$

with α of order 0.5 accounting for the density drop the plasma undergoes before the sheath entrance, and S the collecting surface. Read backwards, this is how the density is extracted in practice: $I_{\mathrm{i,s}}$ from the negatively biased pin and T_e from the triple-probe relation together give n_e.

[8]Note that in a cold plasma, one usually has $T_e \gg T_i$, while in a fully ionized plasma like in a fusion reactor, $T_e \approx T_i$.

Bohm velocity and heat flux. Each charge carrier entering the sheath at c_s also carries energy, so the same criterion sets the heat flux a plasma-facing surface receives:

$$Q_{\mathrm{Bohm}} = \gamma_s \, n_e \, k_B T_e \, c_s \tag{9}$$

where the dimensionless *sheath heat-transmission factor* γ_s corrects for more complex effects: the kinetic energy gained by ions falling through the sheath potential, the energy spectrum of the electrons that make it through, secondary emission. Kinetic theory places it around 7 for typical edge conditions [12], but its exact value depends on the local sheath physics. In this work it is deliberately taken equal to one: the profile analyses of the last part compare pins and plunges *relative to each other*, where a common factor cancels, and the absolute comparison of the camera and Langmuir energies then exposes the effective factor as their measured ratio rather than assuming it.